Performance evaluation of different centrifugal pendulum morphologies through multibody dynamics simulation

Marco Cirelli*

Department of Mechanical Engineering,
University Niccolò Cusano,
Via Don Carlo Gnocchi, 3, 00166 Rome RM, Italy
Email: marco.cirelli@unicusano.it
*Corresponding author

Romualdo Paga, Pier Paolo Valentini and Ettore Pennestrì

Department of Enterprise Engineering,
University of Rome "Tor Vergata",
Via del Politecnico 1, 00133, Italy
Email: romualdopaga@hotmail.it
Email: valentini@ing.uniroma2.it
Email: pennestri@mec.uniroma2.it

Abstract: This paper aims to evaluate the effectiveness of the centrifugal pendulum applied to an internal combustion engine as vibration damper. In particular, a specific design strategy, based on an energy equivalence, is analysed using a series of multibody simulations. A simplified model is initially discussed and different solution morphologies simulated. The present solution is based on the roller-in-slot centrifugal pendulum, designed to have the same kinematic behaviour of lumped mass models. The reasons why the centrifugal pendulum has had in recent years numerous applications are evidenced, together with a discussion of some design strategies. The main characteristics and requirements of this vibration damper are presented. Simulation strategy is subsequently showed, with a description of all bodies, forces and parameters used in the different systems analysed. To assess the effectiveness of the design strategy, a comparison among the simulation results of the different solutions is offered.

Keywords: centrifugal pendulum; vibration absorber; multibody dynamics; trapezoidal pendulum; contact simulation; equivalent mechanism; friction; rollers; passive dampers; torsional vibrations.

Reference to this paper should be made as follows: Cirelli, M., Paga, R., Valentini, P.P. and Pennestrì, E. (2021) 'Performance evaluation of different centrifugal pendulum morphologies through multibody dynamics simulation', *Int. J. Vehicle Performance*, Vol. 7, Nos. 1/2, pp.61–82.

Biographical notes: Marco Cirelli received his BS and MS from the University of Rome Tor Vergata in 2014 and 2016 respectively. In 2020, he received his PhD on Design, Manufacturing, and Operations in Engineering working on multibody dynamics of transmission systems. Currently, he is a

Research Fellow and Lecturer at the University "Niccolò Cusano" in Rome where he teaches the course of Applied Mechanics. His research interests are multibody dynamics, compliant mechanisms, vibration-dampers, structural analysis, optimisation methods, and 3D design methods. He took part in several research projects funded by national and international institutions and industries.

Romualdo Paga received his Bachelor's degree in Mechanical Engineering in 2016, with the thesis on the aerodynamic optimisation of a velomobile through CFD simulations, at the University of Rome Tor Vergata. In 2018, he spent six months study period at the Technische Universität München, where he learned about FEM for car body design, intelligent vehicle systems, and technical acoustics related problems. In 2019, he completed the Master's degree in Mechanical Engineering at the University of Rome Tor Vergata, with the final thesis about multibody dynamic simulations of different embodiments of the centrifugal pendulum to assess its vibration damper properties.

Pier Paolo Valentini complted his MS in Mechanical Engineering and PhD in Design of Mechanical Systems. He is an Associate Professor of Applied Mechanics at the University of Rome Tor Vergata and teaches the courses of Virtual Prototyping and Bioprosthesis. He chairs the Laboratory of Virtual Prototyping and Simulation and serves as Associate Editor for *Mechanism and Machine Theory Journal*, published by Elsevier. His research interests are computational mechanics, virtual prototyping, dynamics, structural simulations, biomechanics, and innovative computer-aided methodologies. He authored more than 160 papers on referred journals and three patents. He coordinated more than 60 research projects funded by national and international institutions and industries.

Ettore Pennestrì received Laurea in Mechanical Engineering (University of Rome, 1980), MS in Mechanical Engineering (Columbia University, 1987), Eng.Sc.D. (Columbia University, 1991). He is currently a Professor of Mechanics of Machines at University of Rome Tor Vergata. His main research interests are kinematics, mechanism design, powertrain analysis, machine dynamics, biomechanics. He authored more than 100 papers in refered journals. In 2018 and 2019, he received the Associate Editor Award for from *ASME Journal of Mechanical Design*. He is a member of the Honorary Editorial Board of Mechanism and Machine Theory.

1 Introduction

The internal combustion engine will continue to play an important role in the mobility with the introduction of new concepts to further reduce fuel consumptions and, consequently, CO_2 emissions. Two development trends, that have already achieved great success and are widely used in current car production, are downsizing, i.e., reduction of the engine size and number of cylinders, and down speeding, i.e., adjustment of transmission ratios to run the engine at lower speeds. Another concept recently introduced to improve engine efficiency is cylinders deactivation. This allows engines to run with half of the cylinders when operating at partial loads. However, all the efficient solutions mentioned increase torsional vibrations in the drivetrain, with strong, low-frequency and high amplitude excitations between the engine and the transmission

(Kooy and Seebacher, 2018). Because of the connected phenomena as discomfort, dynamic amplification, and fatigue issue, torsional vibrations damping is a widely pursued and important topic of scientific investigation. The centrifugal pendulum for vibration absorption (CPVA) is a meaningful solution toward torsional vibrations reduction in rotating machinery (Amburay et al., 2014; Chen and Wu, 2018). This device belongs to the general class of passive vibration dampers, where the damping element (the pendulum) moves as a harmonic oscillator and causes energy transfer from the rotor shaft to the pendulum. However, the addition of such element has a secondary effect on system natural frequencies. The pendulum swing creates a counteracting torque on the rotating shaft and the pendulum oscillation frequency is tuned to suppress a prescribed load torque harmonic component. The CPVA plays an important role to fulfil the challenging NVH requirements of a vehicle and is being adopted by many car manufacturers.

1.1 Historical background

The first CPVA applications on internal combustion engines dates back to the 1930s and 1940s when airplane engine power escalation made clear many vibration-related problems and failures, requiring better damping properties than those offered by the systems already in use. At that time, the automotive industry solution to regularise internal combustion engine power delivery was the single-mass flywheel (SMF), generally coupled with a torsional damper integrated onto the clutch disk. In fact, the adoption of CPVAs in automotive applications was, at that time, hampered by the high mass and large dimensions required to ensure good damping properties (Reik, 1990).

After the 1970s, oil crisis the gradual introduction of more powerful engines, with higher specific torque values, required an improvement of the damping characteristics offered by the SMF. Thus, in the 1980s, the dual-mass flywheel (DMF) was successfully introduced to the market. This device proved to be the most effective solution to dampen higher amplitude torsional vibrations and became the standard for highly compressed diesel and gasoline engines (Reik et al., 1998).

In the 2000s new requirements for improved driving comfort combined with reduced fuel consumption and emissions, together with the progressive adoption of downsizing and down speeding concepts, led the automotive industry to start searching for an even better torsional vibration damping system. A new milestone was set in 2008 with the debut of the DMF with an attached CPVA. This solution, engineered by LuK and initially installed on BMW N47 and Mercedes-Benz OM651 4-cylinder diesel engines, was designed so as to incorporate the CPVA on the secondary flywheel (Zink and Hausner, 2010). In this way, the main issues that prevented the adoption of centrifugal pendulums in car engines were solved. In fact, since vibration levels on the secondary flywheel are already lowered by a significant amount, smaller and lighter pendula could be installed. The solution immediately proved to be superior to any other system already on the market, especially in engine speed range below 2000 rpm where the DMF had a critical behaviour, and rapidly started to be widely used by all the main car manufacturers.

In the next years, many different design concepts were adopted to install CPVAs in combination with manual, torque converter automatic and double-clutch transmissions. In some of most recent applications, the centrifugal pendulum has even completely superseded the DMF; for example, newest 3-cylinder turbocharged gasoline engines have a CPVA directly installed on the clutch disk instead of using a DMF, proving this to be a

more cost-effective solution for smaller and cheaper engines (Kooy, 2014). Nowadays, with a production of over 20 million units in 2018, the CPVA represents the new standard to achieve a superior vibration damping performance for the drivetrain and it is expected to further increase its diffusion in future drivetrain concepts thanks to its exceptional characteristics (Kooy and Seebacher, 2018).

1.2 Design strategies

Several approaches to design CPVAs are discussed in literature. The simplest way is to consider the pendulum as a point-mass (PM-CPVA) attached to the rotor with an ideal link in which gravity effects and Coriolis forces are neglected (Thomson and Dahleh, 1997). This approach allows to easily deduce the equations of motion and consequently the tuning equations for the identification of geometrical and inertial parameters. Silbar and Desoyer extended this first approach to a pendulum with a distributed mass (DM-CPVA) in Silbar and Desoyer (1954). In this work, the equations of motion have been deduced according to Lagrangian formulation. Sibilar and Paslay (1956) deduced the equations of motion of Salomon type CPVA (S-CPVA). This kind of pendulum is realised using a cylindrical mass, called roller, inserted into a cylindrical cavity with a larger radius. Due to the effects of the centrifugal load and to the friction between the pin and the cavity, the rollers roll into the cavity creating the counteracting torque. Another very common typology of CPVA is the bifilar pendulum (B-CPVA). Its distinctive feature is a distributed mass attached to the rotor through two parallel links (Silbar and Desoyer, 1954). In this configuration, the pendulum moves with respect to the rotor only with a translational motion. An equivalence between B-CPVA and PM-CPVA was introduced by Newland in Newland (1964). In this paper the author investigates the non-linear aspects of the vibration behaviour of a B-CPVA. Other studied types of CPVAs are tautochronic pendulums (TAU-CPVA). They have the great advantage to maintain a constant period of oscillation independently from the amplitude. The problem related to the design of TAU-CPVA is the definition of the trajectory with tautochronic condition. Denman (1992) presents a convenient strategy to design TAU-CPVA using a general path representation. The concept of general path means that series of curves as circles, cycloids and epicycloids can be obtained changing only a general parameter. A novel approach to the design of trapezoidal CPVA (T-CPVA) was proposed by Cirelli et al. (2019). T-CPVA has the advantage to exploit the rotational kinetic energy of the pendulum, increasing the damping performance. In order to simplify the design method, an energy equivalence based on the Euler-Savary theory is adopted with the aim to reduce a generic T-CPVA into a PM-CPVA. A design chart approach was finally proposed and comparison with traditional CPVA was made.

1.3 Tuning characteristics

For all the different designs, the tuning condition is respected when local resonance occurs, i.e., when the order of the applied torque is exactly the same as the natural frequency of the tuned pendulum. In this configuration the apparent inertia of the pendulum is infinite with respect to the tuned order of vibration. However, when considering circular paths, a softening nonlinear behaviour is present. This means that the natural frequency of the pendulum decreases with the increase of pendulum amplitude, making the CPVA undertuned at high amplitudes. This has a negative impact on the

damping properties but can be prevented using a small mistuning: the CPVA is intentionally tuned for a slightly different order compared to that of the vibrations that need to be dampened. In general, two types of mistuning are possible:

- Overtuning (positive mistuning): the pendulum is tuned to a higher order than that of the applied torque, thus pushing the excitation point to higher amplitudes. This will delay the nonlinear effects, achieving better performance stability.
- Undertuning (negative mistuning): the pendulum is tuned to a lower order than that of the applied torque, causing instability at lower amplitudes. Obviously, this is an undesired effect and something not recommended because it is counterproductive.

Clearly the resonance tuning is the ideal design option and the one adopted for the simulations in this paper; anyway, for practical reasons, a small overtuning can be used to ensure more stable and reliable operation of the CPVA (Alsuwaiyan and Shaw, 2002).

1.4 Solution morphologies

From a construction point of view, simplified geometries as for example four-bar linkage or simple pendulum cannot be adopted. All the practical solutions are based on the roller-in-slot concept. In details, the system is characterised by roller elements and a generic mass, as showed in Figure 1.

Figure 1 Constructive scheme of general CPVA with exploded view (see online version for colours)

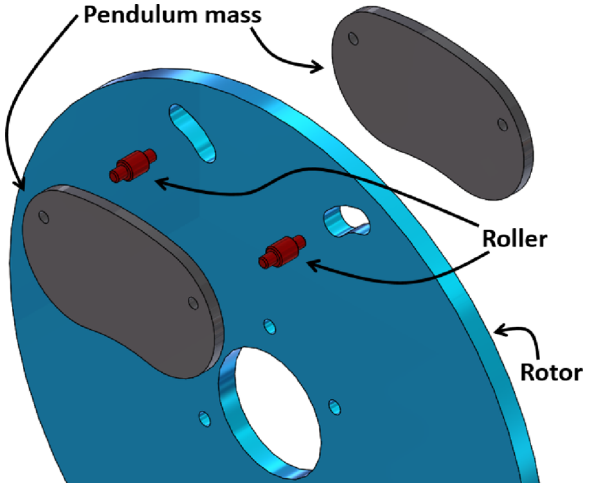

Observing the figure, can be seen that both on the rotor and on the pendulum are visible some slots, in which the roller is located. In this way, a pure rolling motion between roller and rotor is established. With this kind of solution, the dimensioning of the system can be performed according to the stress limit criteria of the pins.

Another important aspect to ensure the correct damping effect of a CPVA is the precision requirements of the slots machining process. This factor plays a decisive role in the system manufacturing; in particular, the pendulum tuning properties are really sensitive to slot radius of curvature errors and, to less extent, also to pendulum centre of

mass location error. This is the reason why high machining accuracy is required to achieve the desired damping performances (Bruce et al., 2018).

Moreover, rollers and slots are the most sensitive areas regarding material wear and tear over time. In particular, wear will most likely occur along the outer surface of the rollers and on the roller slots where contact happens. This generates a small mistuning. Generally, it results in undertuning as the local radius of curvature or the diameter of the rollers change in the centrifugal direction, causing the pendulum to be less effective. A possible solution to this problem is implementing a small overtuning in the design stage to counteract future wear undertuning (Smith, 2015).

1.5 Multibody dynamic simulation strategies

Multibody dynamic simulations allow to investigate the difference of responses for the simplified model adopted for the design and the real constructive morphology.

In this paper, a comparison among different CPVA models is reported. In details, according to the design strategy developed in Cirelli et al. (2019), a comparison between the dynamic behaviour of the T-CPVA, the equivalent PM-CPVA and the constructive system (CS-CPVA) is offered. In order to replicate the effects of the tuning conditions obtained for the T-CPVA using the constructive slot-based solution, a novel methodology for the slot shape design is presented.

2 Multibody models description

A multibody system is made up of different rigid bodies, connected together by means of various joints and couplings. These are used to limit and constrain the movements between the different elements, creating a more complex system. In this way, through dynamic simulations, it is possible to evaluate the behaviour and the interaction of the different rigid bodies of the system under particular motion and/or force conditions. For this reason, the methodology is widely adopted in automotive applications such as cam mechanisms (Valentini and Pennestrì, 2008), gearboxes (Cirelli et al., 2017, 2019) and mechanical joints (Valentini, 2013) in which rotating masses are involved.

2.1 Simplified multibody models: PM-CPVA; T-CPVA

Simplified models are realised without using force-closure couplings. The simplest model is the PM-CPVA (Figure 2) in which the pendulum is connected to the rotor with a revolute joint. The tuning condition (Newland, 1964) allows to identify:

- radius of the installation (r')
- radius of the pendulum (ρ)
- mass of the pendulum (m).

This model introduced many simplifying assumptions not fulfilled in actual embodiments such as absence of friction and negligible inertia of the link between joint and pendulum mass.

Figure 2 PM-CPVA model

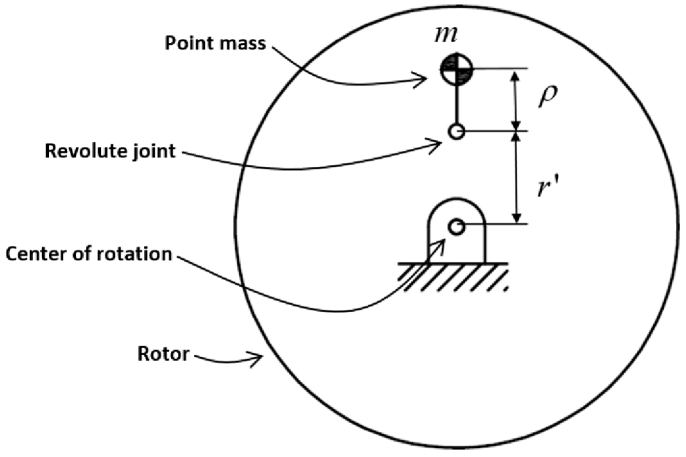

The kinematics of the T-CPVA is equivalent to the one of a four-bar linkage with an attached point mass positioned either directly onto the rod or with an offset with respect to the midpoint of the rod (*d*). From this basic design, two different configurations are possible: one where the rod is shorter than the distance between the two hinges, that has been called convergent T-CPVA; another one where the rod is longer than that distance and is called divergent T-CPVA. The differences between the two shapes are shown in Figure 3 where all the geometrical parameters used in the models are represented.

Figure 3 Convergent (on the left) and divergent (on the right) configuration of the T-CPVA model

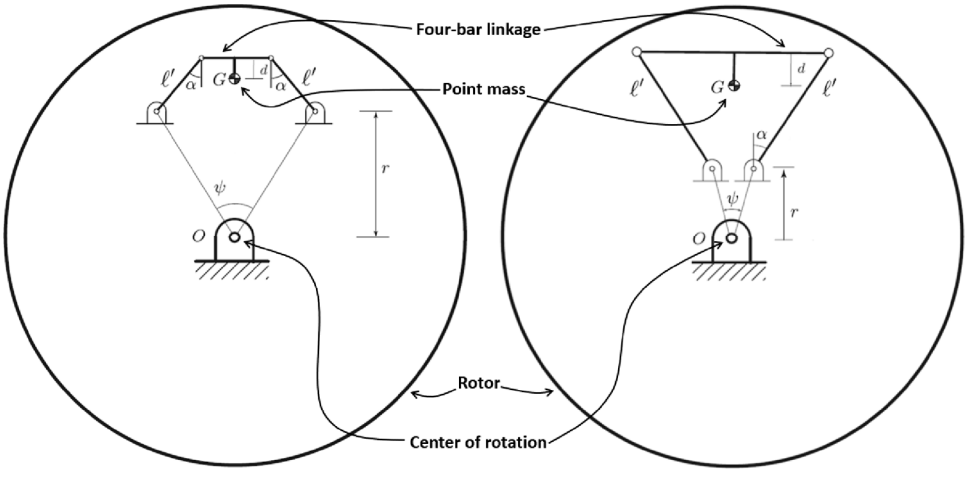

2.2 Constructive solution model CS-CPVA

2.2.1 Geometrical and inertial properties

The actual constructive morphology has more components when compared to the other models. Furthermore, even geometries need to be created in order to satisfy inertial

properties, connections, and so on. For this reason, multibody simulations represent a very powerful methodology to understand the dynamic influence of all parts. It is obvious that elements such as skews, washers, nuts have a limited relevance in the dynamic behaviour, and for this reason can be neglected or assumed rigidly linked to the other bodies. For this study, we have taken into account: the rotor with slots, the rollers and the pendulums.

As can be seen in Figure 4 the pendulum has two circular holes to guarantee the housing of the rollers. As can be observed in the section view, the rollers have three sections of different diameters. The central larger section of the roller, represents the rolling zone where the roller interacts with the rotor slots. This interaction is achieved in multibody model adopting a penalty based contact law with a slip-stick model friction. More detailed description about this formulation is reported in next paragraph. The external sections, with a lower diameter with respect to the central one, are connected to the pendulum through a slipping coupling. This kinematic pair is treated as an ideal revolute joint without friction.

Figure 4 Frontal view with transparent upper pendulum (left) and section view (right) of the CS-CPVA (see online version for colours)

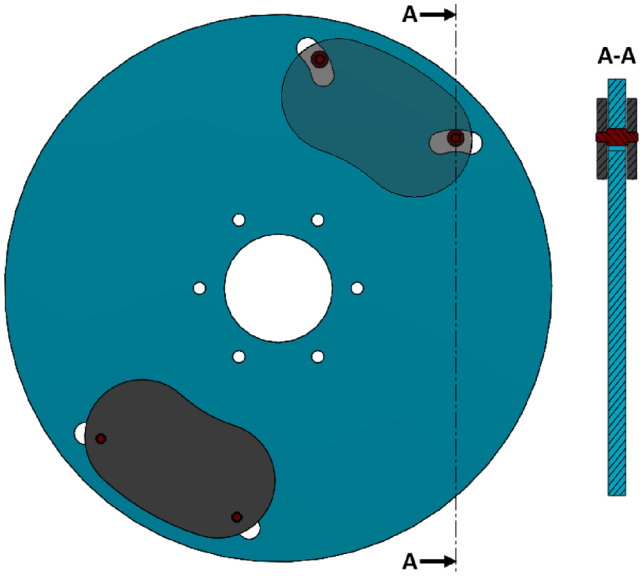

The rotor has two kidney-shaped slots opportunely designed in order to guarantee a correct kinematic of the rollers. With the aim to satisfy this condition, an equivalence between the four-bar linkage of the T-CPVA and the roller-in-slot solution has been considered. According to this analogy, the equivalence condition is satisfied only if the centre of the roller describes a circular trajectory coincident with the *A* end *B* joints trajectories described by the four-bar linkage mechanism (Figure 5). As well as for the T-CPVA also for the CS-CPVA two different models have been created. The first one with convergent geometry and the second with divergent geometry, both based on the corresponding T-CPVA model.

Figure 5 Slots generation based on the four-bar linkage geometry highlighted in yellow (see online version for colours)

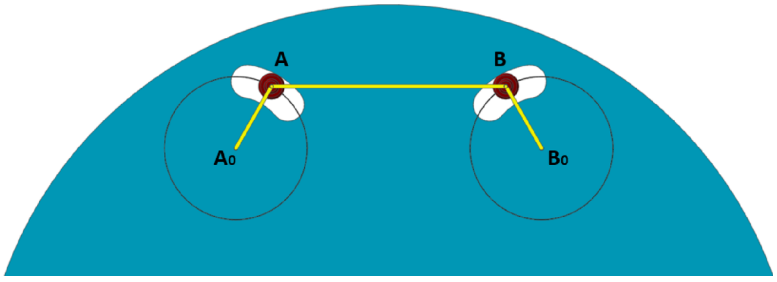

A fundamental parameter to be considered from the equivalence established between the two models is the pendulum lumped inertia. In fact, since the T-CPVA model was tuned considering a lumped mass, the design of the pendulum masses for the constructive model has to keep the inertia at minimum. At the same time, it is of paramount importance to have the mass centre of gravity in the same position as that of the T-CPVA model point mass. For these reasons, a particular cylindrical shape has been chosen (Figure 6). This allows to adjust the pendulum to the tuning value, so as not to compromise the damping characteristics.

Although not included in the simplified model, the roller inertia plays also an important role. It is a very sensitive parameter for the damping properties of the pendulum. Roller mass must be chosen within an appropriate range or the features of the CPVA are negatively compromised.

Figure 6 Front and side view of the cylindrical shaped pendulum (see online version for colours)

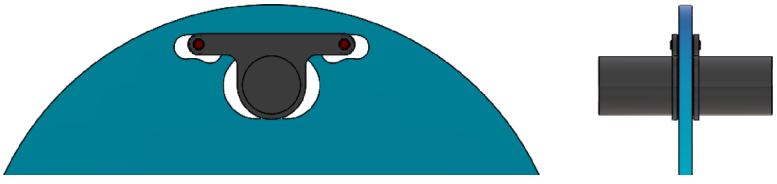

2.2.2 Contact and friction properties

The algorithm adopted for the detection of the contact, is based on a pre-search to identify contact zones, and a detailed-search to find the penetration depth of the contact regions. A more detailed description about the detection method is available in Choi et al. (2010). Since the slots and the rollers are circular profiles, a 2D primitive curves contact model is used. The usage of a 2D contact promote a more accurate estimation of the penetration depth compared with a three-dimensional contact type.

According to the revisited formulation made by Choi et al. (2013), the normal contact force can be calculated using the following relationship:

$$F_n = k_{con}\delta^{m_1} + c_{con}\frac{\dot{\delta}}{|\dot{\delta}|}|\dot{\delta}|^{m_2}\delta^{(m_3)} \tag{1}$$

where δ is the penetration, $\dot{\delta}$ is the penetration speed, k_{con} and c_{con} are respectively the stiffness and the damping coefficients, m_1, m_2 and m_3 are the stiffness, the damping and

the indentation exponents, respectively. This formulation is largely adopted in multibody simulations, e.g., Cirelli et al. (2017) because of its versatility. A stick-slip friction type model is assumed according to the work (Cha et al., 2011) in order to catch out the rolling between coupling roller and the rotor. The tangential force is calculated according to Pennestrì et al. (2015) as follows:

$$F_{\mu} = F_{stiction} + F_{sliding} \tag{2}$$

where $F_{stiction}$ and $F_{sliding}$ represent the friction force during stiction and sliding phase. These contributes can be evaluated as

$$F_{stiction} = -(1-\beta)\mu_s F_n \operatorname{sgn}(\Delta) \tag{3}$$

$$F_{sliding} = -\mu_d F_n \operatorname{sgn}(v) \tag{4}$$

where Δ represents the stiction deformation, β is a parameter depending on the velocity, v is the sliding velocity, μ_d is the dynamic/sliding friction coefficient and μ_s is the static/stiction friction coefficient.

It is crucial to identify values of $\Delta_{\max}$ and v_t that represent the maximum value of the stiction deformation and the threshold velocity respectively. As can be observed from equation (3), $F_{stiction}$ depends on several parameters, summarised in Table 1.

Table 1 Stick-slip parameters in case of either stiction or sliding conditions

State	*Sliding*	*Stiction*
v	$\lvert v\rvert > v_t$	$0 \le \lvert v\rvert \le v_t$
β	1	step $(\lvert v\rvert, -v_t, -1, v_t, 1)$
F_s	0	step $(\lvert F_s\rvert, -\Delta_{\max}, -F_s, \Delta_{\max}, F_s)$
F_d	F_d	step $(\lvert F_d\rvert, -v_t, -F_d, v_t, F_d)$
F	$F_{sliding}$	$F_{stiction} + F_{sliding}$

The step function mentioned in Table 1 regulates the transition from stiction to dynamic conditions and it is expressed as:

$$step(x, x_0, h_0, x_1, h_1) \begin{cases} h_0 & x \le x_0 \\ h_0 + (h_1 - h_0)\left(\dfrac{x - x_0}{x_1 - x_0}\right)^2 \left(3 - 2\left(\dfrac{x - x_0}{x_1 - x_0}\right)\right) & x_0 \le \lvert x\rvert \le x_1 \\ h_1 & x \ge x_1 \end{cases} \tag{5}$$

The contact stiffness between the roller and the other components (pendulum and rotor) is calculated from the Hertz' theory (Puttock and Thwaite, 1969; Young and Budynas, 2002).

Considering the same material for these components, the contact displacement generated from the contact interaction can be calculated from the following relation (Young and Budynas, 2002):

$$v_{contact} = \frac{2F\left(1-\nu^2\right)}{\pi EL}\left(\frac{2}{3}+\ln\left(\frac{2D_1}{b}\right)+\ln\left(\frac{2D_2}{b}\right)\right) \tag{6}$$

where

$$b = \left\{\frac{8F}{\pi L}\left[\frac{1-\nu^2}{E}\right]\frac{D_1 D_2}{D_1 - D_2}\right\}^{\frac{1}{2}} \tag{7}$$

and

- D_1 is the diameter of the slot
- D_2 is the diameter of the roller
- L is the length of the contact
- F is the load applied
- E is the Young Modulus.

Taking into account equations (6) and (7) can be noticed that the relationship between load and displacement is not linear. To find right values for the parameters k_{con} and m_1 to use in equation (1), a fitting of the results from Hertzian analytical solution is performed, considering the magnitude of the load as twice the maximum static load (with the aim to predict the dynamic amplification effect). Regarding the tuning of the other parameters c_{con}, m_2, m_3 that characterise the damping properties of the contact law it has to be considered that the main function of the damping effect is to dissipate energy. In this paper only a preliminary study about the dissipation effect has been done, demonstrating that, within certain limits, damping parameters do not have a relevant influence on the solution. The best option is to tune them to match experiments and achieve a better numerical stability. Anyway, in the simulations all the damping parameters have been conventionally set to the unit value in order to avoid unreal damping effects.

3 Numerical example: tuning condition and sizing of CPVA configurations

To give an overview of the design procedure, a general scheme about the adopted steps has been reported in Figure 7.

Figure 7 adopted workflow

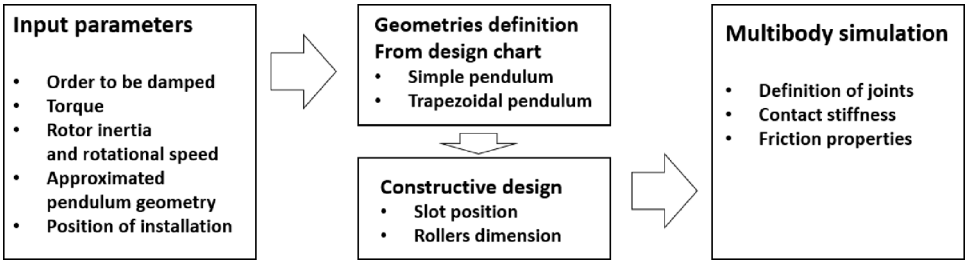

Given a set of the input parameters (the order to be damped, the applied torque, the rotor inertia and its rotational speed, the approximated pendulum geometry and the position of installation), the tuning condition (and consequently the PM-CPVA and T-CPVA geometry) is deduced through the design chart approach, reported in Cirelli et al. (2019). After this step, the equivalent constructive solution is generated considering a feasible shape of the components. Finally, the multibody models have been created and simulated. Figure 8 reports an example of CPVA multibody models created with the described workflow.

Figure 8 Example of CPVA multibody models generated with the explained workflow (see online version for colours)

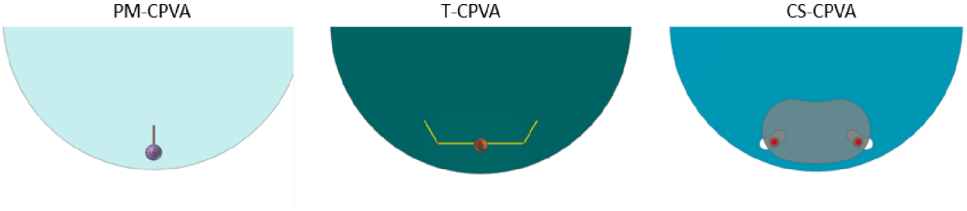

Each of these models has been initially tested with a first order excitation and then with a second order excitation. Finally, the simulations combined both first and second order excitation. To gather experience currently not reported in literature, the convergent and the divergent configurations of both the T-CPVA and the CS-CPVA have been simulated. The simulations involved 15 different cases.

The base system used in the simulations is composed by a rotor with the following characteristics (Mitchiner and Leonard, 1991):

- weight of 9.74 kg
- rotating inertia of 60.000 kg mm^2
- radius of 111 mm
- rotational speed of 875 rpm

The torque values used to perturbate the system, respectively for the first order and the second order excitation, are:

- T_1 = 5698 Nmm
- T_2 = 1695 Nmm.

The geometrical and inertial parameters of the pendulum attached to the rotor are shown in Table 2 for the PM-CPVA and the T-CPVA models. These parameters, calculated from the design charts of Cirelli et al. (2019), vary with the order of excitation to damp according to the tuning equations and also differ when considering the convergent or the divergent configuration.

From Table 2 it can be seen that the tuning mass is quite similar for all the morphologies tested. Its value depends on the order to be tuned. Regarding the CS-CPVA it has been designed using the same geometrical and inertial parameters of the T-CPVA. This was made possible by the requirement for the centre of the roller to describe a circular trajectory coincident with that of the joints of the T-CPVA model, as explained

before. After the definition of the size of the roller and the slot, using equation (6), the contact stiffness between rollers and slots and consequently the friction properties are numerically evaluated (Pennestrì et al., 2015).

A summary of all the contact parameters is reported in Table 3.

Table 2 Geometrical and inertial parameters of the models tuned for first and second order perturbation

PM-CPVA first order tuning						
r' (mm)		ρ (mm)			m' (kg)	
36.21		36.21			2.87	
PM-CPVA second order tuning						
r' (mm)		ρ (mm)			m' (kg)	
65.57		16.39			0.417	
Convergent T-CPVA first order tuning						
Ψ (°)	α (°)	d (mm)	l' (mm)	r (mm)	m_G (kg)	I_G (kg mm^2)
40	10	25.03	25.41	72.43	2.87	174.43
Convergent T-CPVA second order tuning						
Ψ (°)	α (°)	d (mm)	l' (mm)	r (mm)	m_G (kg)	I_G (kg mm^2)
40	10	14.12	14.34	81.96	0.417	25.34
Divergent T-CPVA first order tuning						
Ψ (°)	α (°)	d (mm)	l' (mm)	r (mm)	m_G (kg)	I_G (kg mm^2)
40	–10	25.04	50.85	46.45	2.94	178.78
Divergent T-CPVA second order tuning						
Ψ (°)	α (°)	d (mm)	l' (mm)	r (mm)	m_G (kg)	I_G (kg mm^2)
40	–10	9.76	19.83	75.47	0.385	23.43

Table 3 Summarisation of contact parameters

Normal contact force parameters			*Friction parameters*		
Coefficient	*Value*	*UoM*	*Coefficient*	*Value*	*UoM*
Stiffness	240,000	[N/mm]	μ_s	0.3	
$m1$	1.08		μ_d	0.2	
Damping	1	[N s/mm]	v_t	10	[mm/s]
$m2$	1		$\Delta_{\max}$	0.1	[mm]
$m3$	2				

At this stage, all the CPVA configurations have been defined and the multibody simulations can be executed.

4 Numerical example: dynamic conditions

The dynamic study is performed according to the following considerations: at the beginning of the simulation, all the components of the system have a constant angular velocity ω_0; a perturbation of the system is introduced considering a variable torque expresses as follows:

$$T(t) = \sum_{i=1,2..} T_i \sin(i\omega_0 t) \tag{8}$$

The harmonic amplitude of the load is introduced through a ramp method in order to give a smooth step of excitation. An example of torque load with respect to the time in a transient period of 5 s is shown in Figure 9.

Figure 9 Sinusoidal torque perturbation gradually increasing to the maximum value with a 5 s ramp

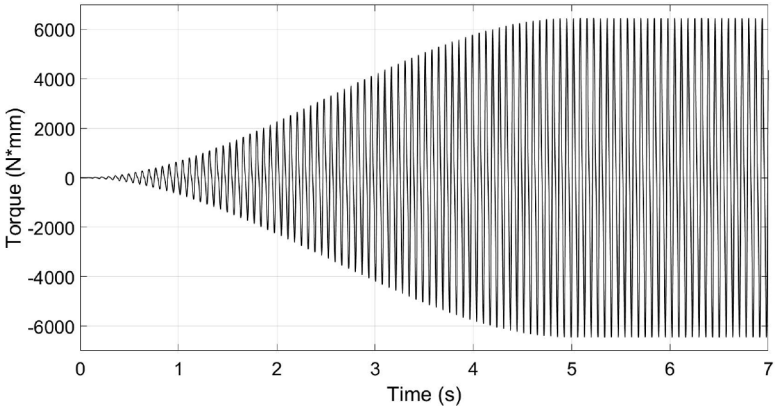

In this investigation, two cases are presented. In the first one the system has only one vibration perturbance to be absorbed. Thus, amplitudes created from only one harmonic need to be reduced. The second one considers a system has two different vibration absorbers in order to reduce vibratory perturbances with two multiple order harmonics. With the aim to maintain a balanced system, for every order, for each CPVA there is one symmetrically mounted on the rotation axis.

The simulation time is set to 40 s to evaluate the transient behaviour of the system, giving it enough time to stabilise after the initial perturbation.

Finally, the numerical integration method used in the simulations is a double-precision differential algebraic system solver (DDASSL). It is explicitly designed for the numerical solution of implicit systems of differential/algebraic equations occurring in the dynamic analysis of mechanical systems (Petzold, 1982). The maximum time step used in the calculation is 10^{-4} seconds and the adopted error tolerance, which represents the maximum size of the error for the solver, is set to 5×10^{-6}.

4.1 First order harmonic damping

The first part of the analysis is dedicated to the reduction of vibrations with only a single-order harmonic. Thus the external torque on the rotor is:

$$T(t) = T_1 \sin(\omega_0 t)$$

The torque is applied with a step function that progressively increases the initial zero torque value to that of $T(t)$ within a timeframe of 5 seconds (Figure 9). This first-order excitation leads to peaks of about 95 rad/s^2 at 14.58 Hz for the angular acceleration of the undamped rotor (Figure 10).

Due to the higher rotor acceleration values and also because of the high total mass required for the first order tuning, eight pendula have been used for the CS-CPVA model. Instead, in the other two simpler models which consider concentrated masses, two pendula have been used. The second run of simulations was performed applying to the flywheel a torque corresponding to a first- order perturbation. Again, a step function is used to gradually increase the torque level from the initial zero value to the full value $T(t)$ that, according to equation (8) is:

$$T(t) = T_2 \sin(2\omega_0 t)$$

The resulting angular acceleration values registered on the undamped rotor are lower when compared to that obtained with the first order perturbation, reaching peaks of up to 25 rad/s^2 at 29.17 Hz (Figure 11).

Figure 10 Undamped rotor acceleration values with first order harmonic perturbation

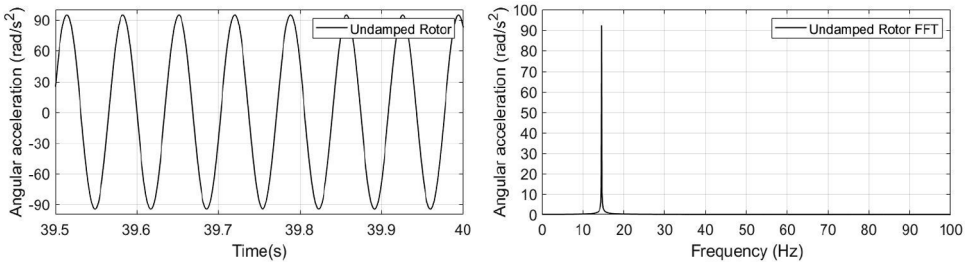

Figure 11 Undamped rotor acceleration values with second order harmonic perturbation

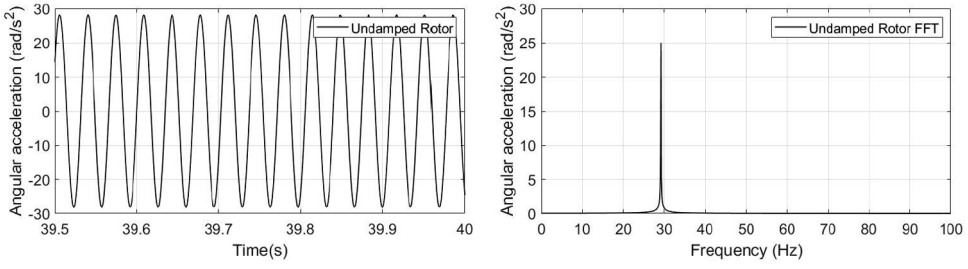

To regularise this acceleration trend each CPVA model has been provided with two masses tuned together for the second order and placed on the rotor symmetrically to the rotation axle.

4.2 Second order harmonic damping

For the last part of the study, simulation runs have been launched considering an external torque that causes to the system both first and second order vibrations. This case of the

study is of particular interest to evaluate the behaviour of different order pendula acting together and to enlighten interactions between them.

In this case, each CPVA model has been provided with some masses to dampen the first-order excitation and some other masses to dampen the second-order excitation, creating a combination of the previous CPVA configurations. Therefore, the geometrical and inertial parameters of the pendula and, consequently, their positioning and their characteristics, are the same showed before for the corresponding order of tuning. Moreover, all the pendula of the same order have been again arranged on the rotor symmetrically to the flywheel axis of rotation.

The torque acting on the rotor is the sum of the torques used in the previous single order simulations, so, according to equation (8):

$$T(t) = T_1 \sin(\omega_0 t) + T_2 \sin(2\omega_0 t)$$

The step function used to gradually increase the torque values is also the same with a five seconds transition. With this torque configuration, the simulated acceleration values on the undamped rotor reach peaks of more than 100 rad/s^2 (Figure 12). From the FFT graph, it can also be observed the different contribution to the final acceleration values respectively of the first (14.58 Hz) and of the second order (29.17 Hz) excitation components.

Figure 12 Undamped rotor acceleration values with first and second order harmonic perturbation

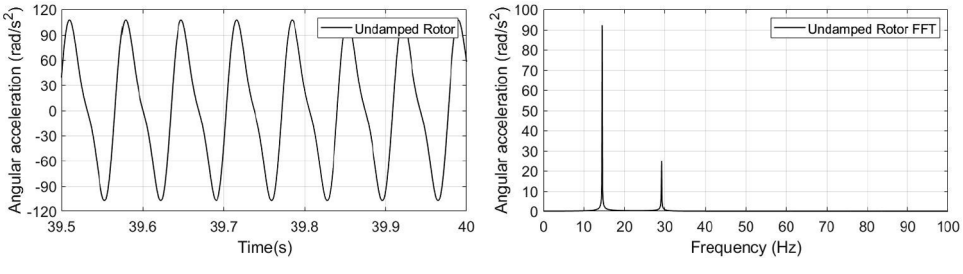

5 Results and discussion

For all the models herein considered, the simulations results are reported both in the time and frequency domains.

To define the attenuation the following index of merit is introduced:

$$\%Att = \frac{\left(\sum_{j=1}^{N} A_j - \sum_{i=1}^{n} A_i\right)}{\sum_{j=1}^{N} A_j} \times 100 \tag{9}$$

where A_j is the *j*th amplitude of vibration of the undamped system and A_i is the amplitude *i*th amplitude of the vibration with the CPVA. The results are divided in three sets of plots, each for every different excitation applied to the system. The first set of plots shows the damping effect obtained for the first order excitation. Both the convergent (Figure 13) and the divergent (Figure 14) configurations are compared to the ideal point-mass pendulum.

Figure 13 Results for the PM-CPVA, convergent T-CPVA and convergent CS-CPVA models with a first-order harmonic excitation

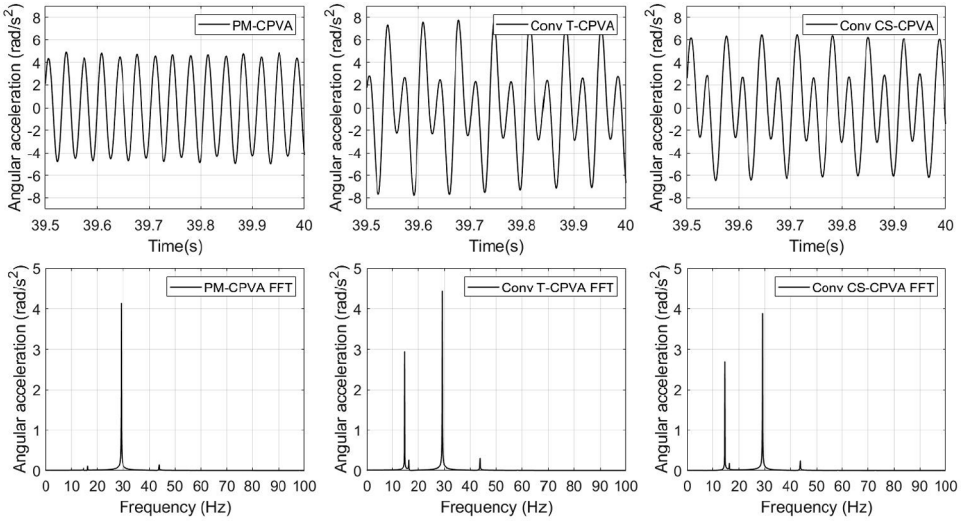

Figure 14 Results for the PM-CPVA, divergent T-CPVA and divergent CS-CPVA models with a first-order harmonic excitation

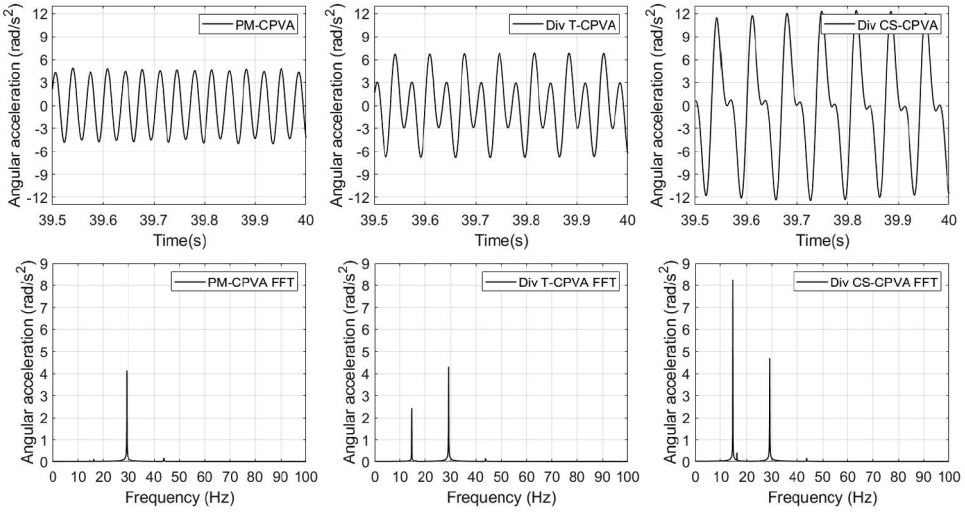

The PM-CPVA models, both in convergent and divergent case, dampen the first order excitation in a satisfactory manner. As a side effect, a small magnitude second order vibration on the rotor is introduced. This is observed in the FFT plot with an acceleration peak at 29.17 Hz. In both cases, an attenuation of 96% is reported. With the convergent configuration it is evident how CONV-T-CPVA and CONV-CS-CPVA models show a very similar damping behaviour, both being able to reduce the angular acceleration of the rotor by an order of magnitude (92% of attenuation). The Divergent configuration DIV-T-CPVA model shows better performances with 93% attenuation of acceleration amplitude, whereas such attenuation is limited to the 86% for the DIV-CS-CPVA

configuration. For this case, deterioration of damping features is mainly due to rollers inertia. We conclude that with this configuration the inertia has a greater influence on the results than in the convergent model. If the DIV-T-CPVA appears to maintain a better performance with respect the CONV-CPVA, the relative constructive solution highlights a worst performance.

Regarding the reduction of second order harmonic, the time and frequency domain responses of the different models discussed are summarised in the plots of (Figure 15) and (Figure 16) for the Convergent and the Divergent configurations, respectively.

Figure 15 Results for the PM-CPVA, convergent T-CPVA and convergent CS-CPVA models with a second-harmonic order excitation

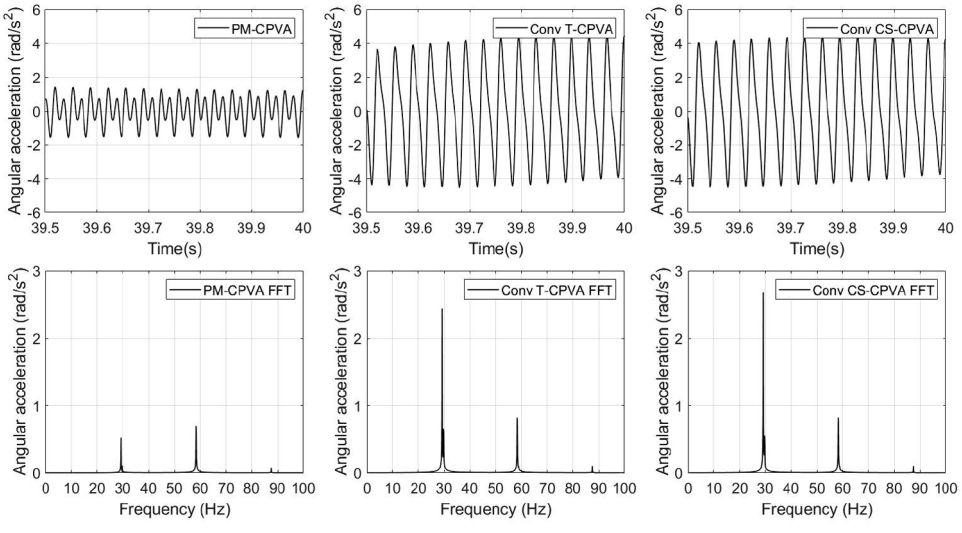

Figure 16 Results for the PM-CPVA, divergent T-CPVA and divergent CS-PVA models with a second-order harmonic excitation

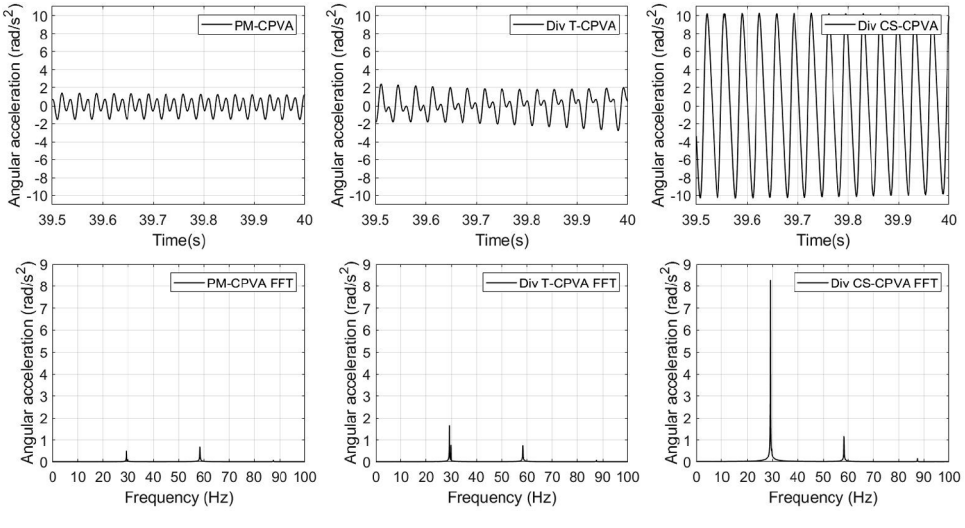

The PM-CPVA model completely dampens the second order excitation (96% attenuation) but, it introduces a small magnitude fourth order vibration on the rotor. This is well visible in the FFT diagram with the acceleration peak at 58.34 Hz. In the convergent models, both CONV-T-CPVA and CONV-CS-CPVA have, as for the previous case, a similar damping behaviour (85% attenuation), although this time the damping effect is less accentuated. The Divergent configuration again attains a satisfactory performance of the corresponding DIV-T-CPVA with a 90% attenuation, but worsened damping for the CS-CPVA model with a 62% attenuation) However, in this case, the inertia of the rollers has a bigger influence on the final solution because the total pendulum inertia is less than that obtained from the first order tuning condition. Moreover, the second order tuning requires a smaller total inertia compared to the first order. Thus the roller inertia has, in proportion, a greater influence.

Finally, the results of the simulations with first and second order excitations combined are reported in the plots of Figures 17 and 18 for the convergent and divergent configurations, respectively.

Figure 17 Results for the PM-CPVA, convergent T-CPVA and convergent CS-CPVA models considering first and second order harmonic excitation combined

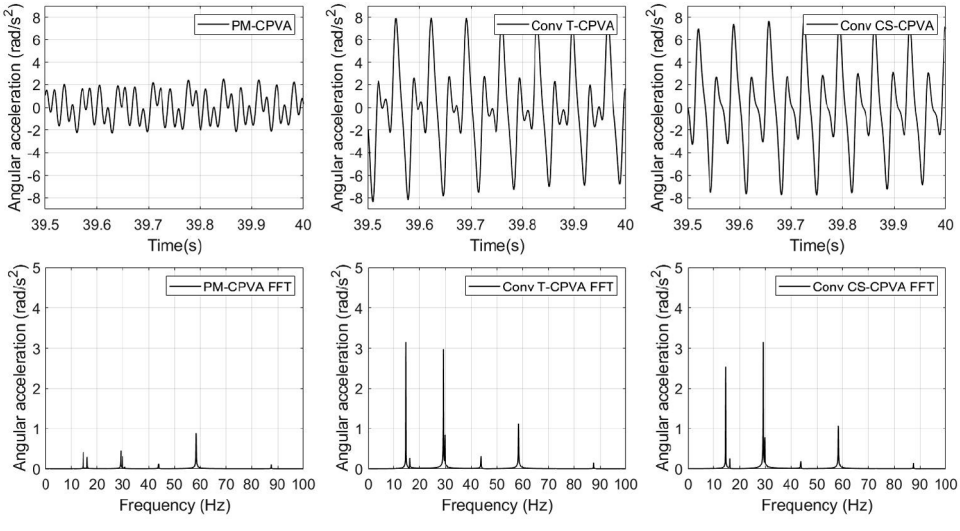

The results show how the combination of two CPVAs, each of them tuned for a different harmonic order, can bring satisfactory results also for the simultaneous damping of two harmonic order excitations. The PM-CPVA is the best performing model, very small residual vibration levels. The remaining two models perform quite well too, confirming that the constructive model can reliably replicate the theoretical convergent trapezoidal configuration on which is based.

For the divergent case with double-excitation the T-CPVA shows a substantially unaltered behaviour compared to the convergent model. On the other side, the CS-CPVA has a compromised damping effect with accelerations levels around three times higher than that found for the convergent model despite the same applied torque. This result was somehow expected considering what was previously found for the other divergent models with single order perturbation.

Figure 18 Results for the PM-CPVA, divergent T-CPVA and divergent CS-CPVA models considering first and second order harmonic excitation combined

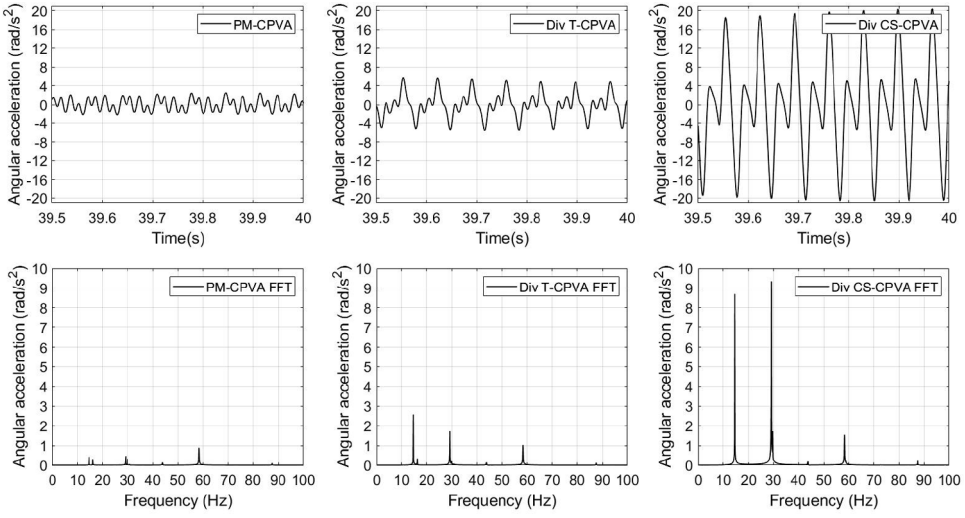

6 Conclusions

In this paper, an analysis regarding the adoption of CPVAs for reducing internal combustion engine vibration of the main shaft has been performed. The analysis is based on nonlinear multibody models. Starting from simplified kinematically equivalent embodiments, that proved their effectiveness in the simulations, different morphologies have been herein analysed. The CS-CPVA, in its convergent design configuration, shows promising damping properties. Conversely, the divergent configuration is not as effective. In this case, the influence of the pendulum inertia and the damping parameters of the contact law require further investigations to find a more accurate model setup.

The double-pendulum configuration also presents a satisfying behaviour. The ability to simultaneously dampen two different orders of vibration could provide a really useful solution for particular applications, such as internal combustion engines with cylinder deactivation technology.

References

Alsuwaiyan, A. and Shaw, S. (2002) 'Performance and dynamic stability of general-path centrifugal pendulum vibration absorbers', *Journal of Sound and Vibration*, Vol. 252, No. 5, pp.791–815.

Amburay, K., Po, S.S. and Rajamohan, V. (2014) 'Design and analysis of a centrifugal absorber for suppression of helicopter blade vibration', *International Journal of Structural Engineering*, Vol. 5, No. 1, pp.24–42.

Bruce, G., Venkatanarayanan, R., Pradeep, A. and William, R. (2018) 'Precision requirements for the bifilar hinge slots of a centrifugal pendulum vibration absorber', *Precision Engineering*, Vol. 52, pp.1–14.

Cha, H., Choi, J., Ryu, H. and Choi, J. (2011) 'Stick-slip algorithm in a tangential contact force model formulti-body system dynamics', *Journal of Mechanical Science and Technology*, Vol. 25, pp.1687–1694.

Chen, D. and Wu, G. (2018) 'Mathematical modelling and simulation of epicycloidal path type centrifugal pendulum vibration absorber applied on three-staged stiffness clutch damper', *International Journal of Vehicle Performance (IJVP)*, Vol. 4, No. 2, pp.115–132.

Choi, J., Rhim, S. and Choi, J.H. (2013) 'A general purpose contact algorithm using a compliance contact force model for rigid and flexible bodies of complex geometry', *International Journal of Non-Linear Mechanics*, Vol. 53, pp.12–23.

Choi, J., Ryu, H.S., Kim, C.W. and Choi, J.H. (2010) 'An efficient and robust contact algorithm for a compliant contact force model between bodies of complex geometry', *Multibody Syst. Dyn.*, Vol. 23, pp.99–120.

Cirelli, M., Valentini, P.P. and Pennestrì, E. (2017) 'Multibody dynamics of gear pairs: comparison among different models', *Proceedings of the 8th ECCOMAS Thematic Conference on Multibody Dynamics*, Prague, pp.255–268.

Cirelli, M., Valentini, P.P. and Pennestrì, E. (2019) 'A study of the non-linear dynamic response of spur gear using a multibody contact based model with flexible teeth', *Journal of Sound and Vibration*, Vol. 445, pp.148–167.

Cirelli, M., Valentini, P.P., Pennestrì, E. and Gregori, J. (2019) 'A design chart approach for the tuning of parallel and trapezoidal bifilar centrifugal pendulum', *Mechanism and Machine Theory*, Vol. 140, pp.711–729.

Denman, H.H. (1992) 'Tautochronic bifilar pendulum torsion absorbers for reciprocating engines', *Journal of Sound and Vibration*, Vol. 159, No. 2, pp.251–277.

Kooy, A. (2014) 'Isolation is the key: the evolution of the centrifugal pendulum-type absorber not only for DMF', *Schaeffler Symposium book 2014*, Schaeffler Technologies AG & Co. KG, Germany, pp.78–93.

Kooy, A. and Seebacher, R. (2018) 'Best-in-class dampers for every driveline concept', *Schaeffler Symposium 2018*, Schaeffler Technologies AG & Co. KG, Germany, pp.146–161.

Mitchiner, R.G. and Leonard, R.G. (1991) 'Centrifugal pendulum vibration absorbers – theory and practice', *Journal of Vibration and Acoustic*, Vol. 113, pp.503–5007.

Newland, D. (1964) 'Nonlinear aspects of the performance of centrifugal pendulum vibration absorbers', *Journal of Engineering for Industry*, Vol. 86, No. 3, pp.257–263.

Pennestrì, E., Rossi, V., Salvini, P. and Valentini, P.P. (2015) 'Review and comparison of dry friction force models', *Nonlinear Dynamics*, Vol. 83, No. 4, pp.1785–1801.

Petzold, L.R. (1982) *Description of DASSL: A Differential/Algebraic System Solver*, N. p., USA.

Puttock, M.J. and Thwaite, E. G. (1969) *Elastic Compression of Spheres and Cylinders at Point and Line Contact*, National Standards Laboratory Technical Paper No. 25, Melbourne, Australia.

Reik, W. (1990) 'Torsional vibration isolation in the drive train – an evaluative study', *04th LuK Symposium 1990*, Schaeffler Automotive Buehl GmbH & Co. KG, Germany, pp.125–146.

Reik, W., Seebacher, R. and Kooy, A. (1998) 'Dual mass flywheel', *06th LuK Symposium 1998*, Schaeffler Automotive Buehl GmbH & Co. KG, Germany, pp.69–93.

Sibilar, A. and Paslay, P. (1956) 'Optimale Auslegung von Salomon-Schwingungstilgern', *Ingenieur-Archiv*, Vol. 24, pp.182–187.

Silbar, A. and Desoyer, K. (1954) 'Zur Erzielung optimaler Wirkung bei Pendel-Schwingungstilgern', *Ingenieur-Archiv*, Vol. 22, pp.36–44.

Smith, E.K. (2015) *Analysis and Simulation of Centrifugal Pendulum Vibration Absorbers*, KTH, School of Engineering Sciences (SCI), Aeronautical and Vehicle Engineering, Marcus Wallenberg Laboratory MWL Stockholm, Sweden.

Thomson, W.T. and Dahleh, M.D. (1997) *Theory of Vibrations with Applications*, 5th ed., Prentice Hall, Upper Saddle River, NJ, USA.

Valentini, P.P. (2013) 'Effects of the dimensional and geometrical tolerances on the kinematic and dynamic performances of the Rzeppa ball joint', *Proceedings of the Institution of Mechanical Engineers Part D Journal of Automobile Engineering*, Vol. 228, pp.37–49.

Valentini, P.P. and Pennestrì, E. (2008) 'Design and simulation of a variable-timing variable-lift cam mechanism', *Proceedings of the Institution of Mechanical Engineers Part D Journal of Automobile Engineering*, Vol. 223, No. 9, pp.1179–1185.

Young, W.C. and Budynas, R.G. (2002) *Roark's Formulas for Stress and Strain*, McGraw-Hill, New York.

Zink, M. and Hausner, M. (2010) 'LuK clutch systems and torsional dampers – key elements for efficient drive trains', *Schaeffler Symposium 2010*, Germany, pp.8–27.